ADVANCED MATERIALS

DOI: 10.1002/adma.200601020

A High-Light-Harvesting-Efficiency Coumarin Dye for Stable Dye-Sensitized Solar Cells**

By *Zhong-Sheng Wang*,* *Yan Cui*, *Kohjiro Hara*,* *Yasufumi Dan-oh*, *Chiaki Kasada*, and *Akira Shinpo*

Dye-sensitized solar cells[1] (DSSCs) have been studied extensively as potential alternatives to conventional inorganic solid solar cells, by using wide-bandgap nanocrystalline TiO_2 sensitized with ruthenium polypyridine complexes[2–6] or metal-free organic dyes[7–12] as photoelectrodes. Through molecular design, ruthenium complexes have achieved power-conversion efficiencies of over 11 %,[2,3,13] while metal-free organic dyes have reached ca. 9 % power-conversion efficiency under AM 1.5 (AM: air mass) simulated solar light of 100 mW cm^{-2} (1 sun).[14,15] Several ruthenium polypyridyl complexes have shown their ability to withstand thermal or light-soaking stress tests for at least 1000 h while retaining an efficiency above 7 %,[16–18] whereas for organic-dye-based DSSCs the long-term stability, which is the critical requirement for practical applications, so far remains a serious problem.

Organic dyes are also promising for applications in DSSCs in that they have much higher molar extinction coefficients[19–21] than those for ruthenium polypyridine complexes, which are favorable for light-harvesting efficiency (LHE) and hence photocurrent generation. Among the organic dye sensitizers tested in DSSCs, coumarin dyes are strong candidates because of their good photoelectric conversion properties.[8,22] However, one of their drawbacks is that a high concentration of 4-*tert*-butylpyridine (TBP) is usually required for a high power-conversion efficiency.[22] Under continuous light soaking of 1 sun for a short period of one day, the photovoltaic performance was observed to drop dramatically because of the dissolution of the dye into electrolyte containing 0.5 M or more TBP. Therefore, it still remains a great challenge to acquire a DSSC based on a metal-free organic dye with high efficiency that is stable in the long term. In this paper, we report a new coumarin dye, 2-cyano-3-{5′-[1-cyano-2-(1,1,6,6-tetramethyl-10-oxo-2,3,5,6-tetrahydro-1*H*,4*H*,10*H*-11-oxa-3a-aza-benzo[*de*]anthracen-9-yl)-vinyl]-[2,2′]bithiophenyl-5-yl}-acrylic acid (NKX-2883), shown in Figure 1, for use in DSSCs.

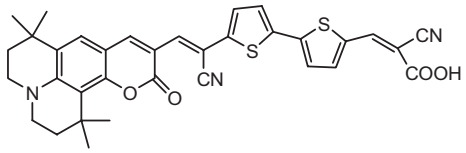

Figure 1. Structure of NKX-2883.

These DSSCs exhibited LHE values of near unity, incident photon-to-electron conversion efficiency (IPCE) over a wide spectral region on transparent TiO_2 films of only 6 μm thickness, and maintained ca. 6 % power-conversion efficiency under continuous light soaking of 1 sun at 50–55 °C for 1000 h.

Figure 2a shows the UV-vis absorption spectrum for NKX-2883 in an ethanol solution. NKX-2883 exhibited two π–π* electron-transition peaks (426 and 552 nm) in the visible region. Compared to NKX-2677 (2-cyano-3-[5'-(1,1,6,6-tetramethyl-10-oxo-2,3,5,6-tetrahydro-1H,4H,10H-11-oxa-3a-aza-benzo[de]anthracen-9-yl)-[2,2']bithiophenyl-5-yl]acrylic acid), one of the best organic dyes for DSSCs reported previously,[22] the introduction of one more CN group into the molecular frame decreases the gap between the highest occupied molecular orbital (HOMO) and the lowest unoccupied molecular orbital (LUMO), thus extending the maximum absorption from 511 to 552 nm. This red-shift may favor light harvesting and hence photocurrent generation in DSSCs, as will be discussed below. The 552 nm peak showed a broad feature with a full width at half-maximum absorbance of ca. 110 nm, comparable to that for ruthenium polypyridyl complexes,[2] contributing broadly to the high LHE. The molar extinction coefficient (ε) of NKX-2883 in ethanol was determined to be 9.74×10^4 dm^3 mol^{-1} cm^{-1} at 552 nm, which is about seven times larger than that of N3 (cis-di(thiocyanate)-bis(2,2'-bipyridyl-4,4'-dicarboxylic acid); $\varepsilon = 1.42 \times 10^4$ dm^3 mol^{-1} cm^{-1} at 532 nm),[2] and 60 % larger than that for NKX-2677 ($\varepsilon = 6.43 \times 10^4$ dm^3 mol^{-1} cm^{-1} at 511 nm).[22] The LUMO (–0.69 V vs the normal hydrogen electrode (NHE)) of NKX-2883 is more negative than the conduction-band edge of TiO_2 (–0.5 V vs NHE),[23] ensuring that electron injection from the excited dye to the conduction band of TiO_2 is thermodynamically favorable.

The dye-loaded films were obtained by dipping the TiO_2 film in dye solutions with different concentrations: 0.02, 0.1, 0.3, and 1.0 mM. The normalized UV-vis absorption spectra for dye-loaded films are plotted in Figure 2b. It is evident that the spectrum becomes slightly broader with an increasing con-

[*] Dr. Z.-S. Wang, Dr. K. Hara, Y. Cui
National Institute of Advanced Industrial Science and Technology (AIST)
1-1-1 Higashi, Tsukuba, Ibaraki 305-8565 (Japan)
E-mail: zs.wang@aist.go.jp; k-hara@aist.go.jp
Y. Dan-oh, C. Kasada, A. Shinpo
Hayashibara Biochemical Laboratories, Inc.
564-176 Fujita, Okayama 701-0221 (Japan)

[**] This work was supported by the Industrial Technology Research Grant Program in 2005 from the New Energy and Industrial Technology Development Organization (NEDO) of Japan.

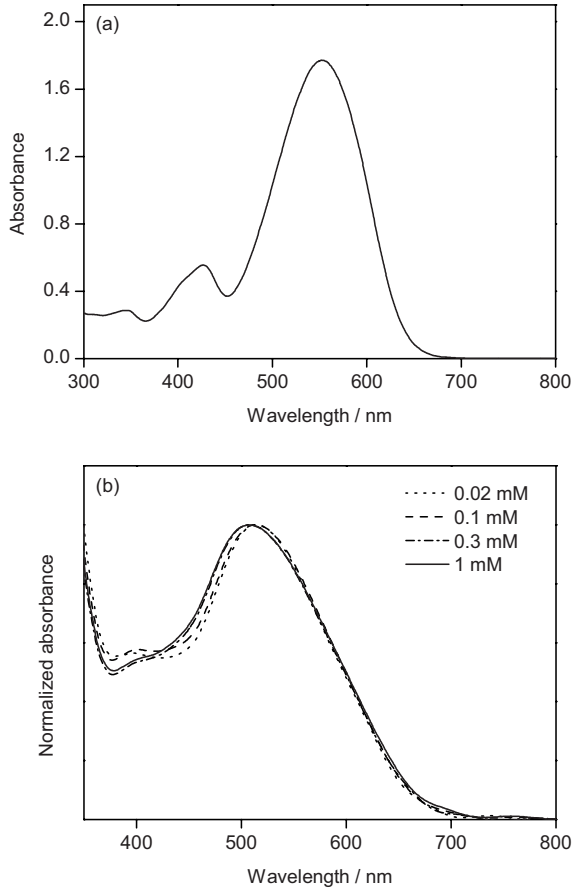

Figure 2. a) UV-vis absorption spectrum of NKX-2883 in ethanol solution and b) normalized spectra for dye-loaded 1.66 μm TiO_2 transparent film, obtained from sensitization in 0.02, 0.1, 0.3, and 1.0 mM dye solutions, respectively.

centration of dye solution. The gradual broadening of the absorption peak with increasing dye concentration is attributed to the π–π stacking of the dye.[21,24,25] A maximum absorbance of 2.3 could be obtained from a dye-loaded transparent TiO_2 film just 1.6 μm thick. When using a 6.0 μm TiO_2 film the maximum absorbance was beyond the upper limit (i.e., 5.0), and an absorbance greater than 1.0, corresponding to >90% of the LHE, was observed in the spectral region below 660 nm. LHE of unity is expected in this spectral region with the assistance of a Pt mirror coating on the counter electrode, which guarantees high IPCE values in a similar spectral region.

The photovoltaic performance of the DSSCs reported in this work was obtained with a nonvolatile electrolyte comprising 0.6 M 1,2-dimethyl-3-*n*-propylimidazolium iodide (DMPImI), 0.1 M I_2, and 0.1 M *N*-methylbenzimidazole (NMBI) in 3-methoxypropionitrile (MPN). This kind of redox electrolyte has been reported to be beneficial for long-term stability[17] but is disadvantageous for cell efficiency. The IPCE action spectrum of NKX-2883 on 6 μm TiO_2 is shown in Figure 3. It exhibits a broad feature with the IPCE onset at 850 nm. From 430 to 660 nm, the IPCE remains almost constant at >80%, corresponding to an IPCE of unity (taking the light loss arising

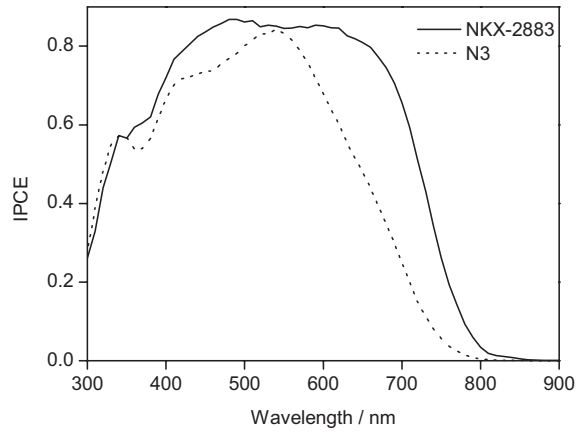

Figure 3. IPCE action spectra for NKX-2883- or N3-loaded 6 μm transparent TiO_2 films, respectively. The electrolyte was 0.6 M DMPImI, 0.1 M I_2, and 0.1 M NMBI in MPN.

from the light absorption and reflection by the conducting glass into account) as a result of unity LHE in a similar spectral region, as seen in Figure 2b. For comparison, the action spectrum of N3 is also presented in Figure 3. It is clear that the action spectrum of NKX-2883 is much broader than that of N3 under the same conditions. The integrated photocurrent densities from the action and global AM 1.5G standard solar emission spectra were estimated to be 14.3 and 19.0 mA cm^{-2} for N3 and NKX-2883, respectively. Only on TiO_2 films of 15 μm or thicker containing scattering particles does N3 exhibit a similar broad feature[26] in its action spectrum to that observed for NKX-2883 on 6 μm film.

Because of the high extinction coefficient and broad absorption feature in the visible region of the NKX-2883-loaded film, it is feasible to produce thin cells with optimal efficiency. A 6 μm TiO_2 film was verified as being optimal for the power-conversion efficiency[27]—its current–voltage characteristics are shown in Figure 4. Under illumination of 100 mW cm^{-2} AM 1.5G simulated solar light, the cell produced a short-cir-

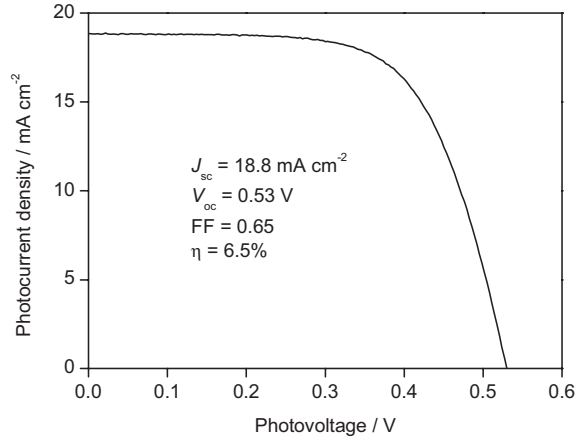

Figure 4. *I–V* curve for a NKX-2883-based solar cell with a mask under 100 mW cm^{-2} illumination from AM 1.5G simulated solar light.

ADVANCED MATERIALS

cuit photocurrent density (J_{sc}) of 18.8 mA cm^{-2}, an open-circuit photovoltage (V_{oc}) of 0.53 V, and a fill factor (*FF*) of 0.65, corresponding to a 6.5 % power-conversion efficiency (η). The J_{sc} obtained is in good agreement with the integrated photocurrent density (19.0 mA cm^{-2}), indicating that the mismatch between simulated light and true light is very small. It is impressive to have obtained such a high photocurrent on such a thin transparent film. To the best of our knowledge, this is the highest photocurrent density reported for DSSCs on transparent films as thin as 6 μm. The obtained value of J_{sc} (18.8 mA cm^{-2}) for NKX-2883 on the 6 μm transparent TiO_2 film is even greater than that for black dye on a 32 μm TiO_2 film (18.3 mA cm^{-2}).[28]

One can see from Figure 4 that the V_{oc} of this dye is only around 0.5 V. If the V_{oc} is optimized, through molecular design and through varying the redox electrolyte composition, to the level of N3, e.g. >0.7 V, ca. 10 % power-conversion efficiency can be anticipated for metal-free organic dyes. It is noteworthy that the power-conversion efficiency of the NKX-2883-based DSSC can be increased to 7.6 % (J_{sc} = 16.5 mA cm^{-2}, V_{oc} = 0.61 V, *FF* = 0.76) by using an acetonitrile electrolyte containing 0.6 M DMPImI, 0.1 M LiI, 0.05 M I_2, and 0.1 M TBP. Compared to the NKX-2677 dye reported previously,[22] which yielded 6.2 % η (J_{sc} = 13.2 mA cm^{-2}, V_{oc} = 0.63 V, FF = 0.75), NKX-2883 produced much higher J_{sc} but slightly lower V_{oc}, resulting in a much higher efficiency under the same conditions. Because this work focuses on the photovoltaic performance and stability for NKX-2883 using a nonvolatile electrolyte, we have not described the details of DSSCs based on the acetonitrile electrolyte here.

Long-term stability is one of the critical parameters limiting cell applications. An NKX-2883-based DSSC in open-circuit mode was subjected to continuous visible-light soaking at 50–55 °C and showed good stability employing a nonvolatile electrolyte, as shown in Figure 5. J_{sc} did not change much for the first 150 h, then increased gradually up to 800 h, followed by a plateau up to 1000 h. Conversely, V_{oc} decreased by only 50 mV, from 0.53 to 0.48 V, while *FF* first increased from 0.72 to 0.74 up to 150 h and then dropped slowly to 0.71, remaining stable from 600 to 1000 h. As a consequence, the power-conversion efficiency increased from 5.9 to 6.2 % and then remained almost constant until 1000 h. As the temperature increases during light soaking, electrolyte diffusion becomes faster and the conduction-band edge moves downward relative to I^-/I_3^-;[29] both effects result in the enhancement of J_{sc} and the latter effect leads to a decrease in V_{oc}. The initial increase in *FF* up to 150 h is also due to the faster electrolyte diffusion as the temperature increases. The stability data shown in Figure 5 indicate that organic dyes also have good photostability, similar to the more frequently used ruthenium polypyridine complexes. The cell in short-circuit mode also showed good stability but with the efficiency decreasing by 5–15 %.

In summary, we have demonstrated a new coumarin dye exhibiting quite a high extinction coefficient and hence producing unity IPCE values in a broad spectral region on a transparent film only 6 μm thick. The high LHE allows a very thin film to be used in the DSSCs, which is important in reducing photovoltage loss due to an increased film resistance and charge recombination; in keeping a relatively high mechanical strength of the film when surrounded by liquid electrolyte during cell operation; and in cutting the total production cost. For the first time, DSSCs with long-term stability based on metal-free organic dyes and with a power-conversion efficiency of ca. 6 % have been fabricated and operated under continuous light-soaking stress for up to 1000 h.

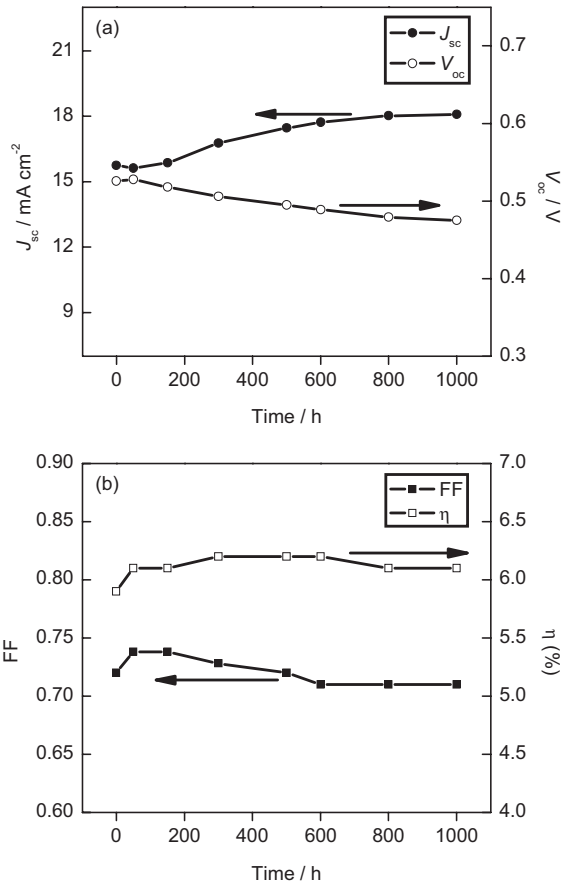

Figure 5. Evolution of solar cell parameters during visible-light soaking (AM 1.5G, 100 mW cm^{-2}) at 50–55 °C. A 420 nm cut-off filter was put on the cell surface during illumination. a) J_{sc} and V_{oc}, b) *FF* and η.

Experimental

Reagents: TBP, NMBI, LiI, and I_2 were purchased from Aldrich. DMPImI was obtained from Tomiyama Pure Chemical Industries Ltd., Japan. All reagents and solvents used in this study were reagent grade and used as received.

Synthesis of NKX-2883: 1,1,6,6-tetramethyl-10-oxo-2,3,5,6-tetrahydro-1H,4H,10H-11-oxa-3a-aza-benzo[de]anthracen-9-carbaldehyde (15 g) and thiophene-2-yl-acetonitrile (30 g) were dissolved in 30 mL *N*,*N*-dimethylformamide (DMF), and then acetic acid (7.9 mL) and piperidine (15.2 mL) were added to the solution, which was kept at 90 °C for 1 h. Thiophene-2-yl-acetonitrile (2.6 mL) was added to the solution, which was stirred at 90 °C for another 30 min. Addition of

methanol (90 mL) to this reaction system followed by cooling afforded crystals of 3-(1,1,6,6-tetramethyl-10-oxo-2,3,5,6-tetrahydro-1*H*,4*H*,10*H*-11-oxa-3a-aza-benzo[de]anthracen-9-yl)-2-thiophene-2-yl-acrylonitrile **1** (11.2 g). ^{1}H NMR ($CDCl_3$) δ (TMS, ppm): 1.31 (6H, s), 1.55 (6H, s), 1.76 (2H, t), 1.81 (2H, t), 3.29 (2H, t), 3.37 (2H, t), 7.05 (1H, d), 7.19 (1H, s), 7.28 (1H, d), 7.33 (1H, d), 7.70 (1H, s), 8.58 (1H, s). **1** (10 g) was dissolved in 150 mL DMF at 40 °C and then 21 mL DMF solution containing 4.2 g *N*-bromosuccinimide was added to this solution, which was stirred for 30 min. After adding methanol (100 mL) to the reaction system followed by cooling, crude crystals of 2-(5-bromo-thiophen-2-yl)-3-(1,1,6,6-tetramethyl-10-oxo-2,3,5,6-tetrahydro-1H,4H,10H-11-oxa-3a-aza-benzo[de]anthracen-9-yl)acrylonitrile **2** (9.5 g) were obtained. The crude crystals of **2** were purified by recrystallization from DMF (6.5 g). ^{1}H NMR ($CDCl_3$) δ (TMS, ppm): 1.30 (6H, s), 1.54 (6H, s), 1.71–1.83 (4H, m), 3.27–3.31 (2H, m), 3.36–3.40 (2H, m), 7.00 (1H, d), 7.06 (1H, d), 7.18 (1H, s), 7.57 (1H, s), 8.56 (1H, s). **2** (6.5 g), 2-thiopheneboronic acid (2.1 g), tetrakis(triphenylphosphine)palladium(0) ($Pd(PPh_3)_4$, 0.44 g), and K_2CO_3 (5.3 g) were dissolved in 130 mL DMF and then kept at 120 °C for 4.5 h under an Ar atmosphere. 1.1 g 2-thiopheneboronic acid and 0.22 g $Pd(PPh_3)_4$ were added to the solution and then kept for 2.5 h. After filtration of the solution, crystals of 2-[2,2′]bithiophenyl-5-yl-3-(1,1,6,6-tetramethyl-10-oxo-2,3,5,6-tetrahydro-1H,4H,10*H*-11oxa-3a-aza-benzo[de]anthracen-9-yl)-acrylonitrile **3** (4.6 g) were obtained from the filtrate. ^{1}H NMR ($CDCl_3$) δ (TMS, ppm): 1.31 (6H, s), 1.55 (6H, s), 1.74 (2H, t), 1.82 (2H, t), 3.32 (2H, t), 3.41 (2H, t), 7.19 (1H, s), 7.40 (1H, d), 7.70 (1H, d), 7.93 (1H, s), 8.67 (1H, s), 9.87 (1H, s). **3** (4 g) was dissolved in 120 mL DMF and then Vilsmeyer reagent, prepared from 22 mL DMF and 7.3 mL phosphorus oxychloride, was added to the solution, which was kept at 70 °C for 4 h (Vilsmeyer–Haack reaction). After cooling to 10 °C, the resultant solution was added to 750 mL iced water. After neutralization with 25 % NaOH solution, the resultant precipitates were washed with methanol (60 mL). Recrystallization of the precipitates from chloroform and methanol afforded crystals of 2-(5′-formyl-[2,2′]bithiophenyl-5-yl)-3-(1,1,6,6-tetramethyl-10-oxo-2,3,5,6-tetrahydro-1*H*,4*H*,10*H*-11-oxa-3a-aza-benzo[de]anthracen-9-yl)-acrylonitrile **4** (1.5 g). ^{1}H NMR ($CDCl_3$) δ (TMS, ppm): 1.31 (6H, s), 1.56 (6H, s), 1.72–1.84 (4H, m), 3.29–3.33 (2H, m), 3.37–3.41 (2H, m), 7.19 (1H, s), 7.26–7.33 (3H, m), 7.68 (1H, d), 7.72 (1H, s), 8.61 (1H, s), 9.87 (1H, s). **4** (0.7 g) and cyanoacetic acid (0.17 g) were refluxed in chloroform (14 mL) in the presence of piperidine (0.04 mL) for 1 h. Recrystallization of the resultant precipitates (0.74 g) from chloroform–triethylamine mixed solvent by adding acetic acid and acetonitrile afforded crystals (0.52 g) of NKX-2883. ^{1}H NMR (DMSO-d_7) δ (TMS, ppm): 1.27 (6H, s), 1.47 (6H, s), 1.7–1.8 (4H, m), 3.3–3.4 (4H, m), 7.38 (1H, d), 7.40 (1H, s), 7.60 (1H, s), 7.61 (1H, d), 7.66 (1H, d), 7.97 (1H, d), 8.47 (1H, s), 8.52 (1H, s). Electron-ionization mass spectrometry (MS-EI): *m*/*z* 606.05, $(M\text{-}H)^-$. Analytical calculation for $C_{34}H_{29}N_3O_4S_2{\cdot}H_2O$: C, 65.26 %; H, 4.99 %; N, 6.72 %; S, 10.25 %. Found: C, 65.33 %; H, 4.66 %; N, 6.28 %; S, 9.62 %.

Fabrication of Solar Cells: 6 μm transparent films composed of 23 nm nanoparticles[26] were fabricated on conducting glass (transparent conducting oxide (TCO), F–SnO_2, 10 Ω/□, Nippon Sheet Glass Co., Japan) by using a screen-printing method. TiO_2 films were sensitized by dipping in a 0.3 mM solution of NKX-2883 in ethanol for ca. 12 h. The hermetically sealed cells were fabricated by assembling the dye-loaded film as the working electrode and Pt-coated TCO glass as the counter electrode separated with a hot-melt surlyn film (30 μm), as described previously[30]. Solar cells (apparent active area was 0.25 cm^2) were evaluated with IPCE action spectra and *I*–*V* curves with a metal mask (aperture area was 0.2354 cm^2) on the cell surface to avoid diffusive light. The sealed cell with a 420 nm cut-off filter on the cell surface at open-circuit was subject to continuous light soaking (100 mW cm^{-2} AM 1.5 simulated solar light, cell surface temperature 50–55 °C).

Received: May 5, 2006
Revised: October 26, 2006
Published online: March 20, 2007

[1] B. O'Regan, M. Grätzel, *Nature* **1991**, *353*, 737.
[2] M. K. Nazeeruddin, A. Kay, I. Rodicio, R. Humphry-Baker, E. Müller, P. Liska, N. Vlachopoulos, M. Grätzel *J. Am. Chem. Soc.* **1993**, *115*, 6382.
[3] M. K. Nazeeruddin, P. Pechy, T. Renouard, S. M. Zakeeruddin, R. Humphry-Baker, P. Comte, P. Liska, C. Le, E. Costa, V. Shklover, L. Spiccia, G. B. Deacon, C. A. Bignozzi, M. Grätzel, *J. Am. Chem. Soc.* **2001**, *123*, 1613.
[4] H. Zabri, I. Gillaizeau, C. A. Bignozzi, S. Caramori, M.-F. Charlot, J. Cano-Boquera, F. Odobel, *Inorg. Chem.* **2003**, *42*, 6655.
[5] Z.-S. Wang, C.-H. Huang, B.-W. Zhang, Y.-J. Hou, P.-H. Xie, H.-J. Qian, K. Ibrahim, *New J. Chem.* **2000**, *24*, 567.
[6] A. Hagfeldt, M. Grätzel, *Acc. Chem. Res.* **2000**, *33*, 269.
[7] Z.-S. Wang, F.-Y. Li, C.-H. Huang, *Chem. Commun.* **2000**, 2063.
[8] K. Hara, T. Sato, R. Katoh, A. Furube, Y. Ohga, A. Shinpo, S. Suga, K. Sayama, H. Sugihara, H. Arakawa, *J. Phys. Chem. B* **2003**, *107*, 597.
[9] Z.-S. Wang, K. Sayama, H. Sugihara, *J. Phys. Chem. B* **2005**, *109*, 22 449.
[10] T. Kitamura, M. Ikeda, K. Shigaki, T. Inoue, N. A. Anderson, X. Ai, T. Lian, S. Yangagida, *Chem. Mater.* **2004**, *16*, 1806.
[11] D. P. Hagberg, T. Edvinsson, T. Marinado, G. Boschloo, A. Hagfeldt, L. Sun, *Chem. Commun.* **2006**, 2245.
[12] S.-L. Li, K.-J. Jiang, K.-F. Shao, L.-M. Yang, *Chem. Commun.* **2006**, 2792.
[13] Y. Chiba, A. Islam, Y. Watanabe, R. Komiya, N. Koide, L. Han, *Jpn. J. Appl. Phys.* **2006**, *45*, L638.
[14] T. Horiuchi, H. Miura, K. Sumioka, S. Uchida, *J. Am. Chem. Soc.* **2004**, *126*, 12 218.
[15] S. Ito, S. M. Zakeeruddin, R. Humphry-Baker, P. Liska, R. Charvet, P. Comte, M. K. Nazeeruddin, P. Péchy, M. Takata, H. Miura, S. Uchida, M. Grätzel, *Adv. Mater.* **2006**, *18*, 1202.
[16] P. Wang, S. M. Zakeeruddin, R. Humphry-Baker, J. E. Moser, M. Grätzel, *Adv. Mater.* **2003**, *15*, 2101.
[17] P. Wang, S. M. Zakeeruddin, P. Comte, R. Charvet, R. Humphry-Baker, M. Grätzel, *J. Phys.Chem. B* **2003**, *107*, 14 336.
[18] P. Wang, C. Klein, R. Humphry-Baker, S. M. Zakeeruddin, M. Grätzel, *J. Am. Chem. Soc.* **2005**, *127*, 808.
[19] Z.-S. Wang, F.-Y. Li, C.-H. Huang, *J. Phys. Chem. B* **2001**, *105*, 9210.
[20] Z.-S. Wang, F.-Y. Li, C.-H. Huang, L. Wang, M. Wei, L.-P. Jin, N.-Q. Li, *J. Phys. Chem. B* **2000**, *104*, 9676.
[21] A. Ehret, L. Stuhl, M. T. Spitler, *J. Phys. Chem. B* **2001**, *105*, 9960.
[22] K. Hara, Z.-S. Wang, T. Sato, A. Furube, R. Katoh, H. Sugihara, Y. Dan-oh, C. Kasada, A. Shinpo, S. Suga, *J. Phys. Chem. B* **2005**, *109*, 15 476.
[23] A. Hagfeldt, M. Grätzel, *Chem. Rev.* **1995**, *95*, 49.
[24] Z.-S. Wang, K. Hara, Y. Dan-oh, C. Kasada, A. Shinpo, S. Suga, H. Arakawa, H. Sugihara, *J. Phys. Chem. B* **2005**, *109*, 3907.
[25] K. Hara, M. Kurashige, Y. Dan-oh, C. Kasada, A. Shinpo, S. Suga, K. Sayama, H. Arakawa, *New J. Chem.* **2003**, *27*, 783.
[26] Z.-S. Wang, H. Kawauchi, T. Kashima, H. Arakawa, *Coord. Chem. Rev.* **2004**, *248*, 1381.
[27] When film thickness was below 6 μm, the η and J_{sc} were low because of the low dye adsorption. When film thickness increased from 6 (see Fig. 4) to 12 μm, J_{sc} increased from 18.83 to 19.07 mA cm^{-2}, but V_{oc} and *FF* decreased from 0.530 V and 0.652 to 0.524 V and 0.643, respectively, leading to a slight decrease in η from 6.5 to 6.4 %. Further increasing the film thickness resulted in decreased efficiency because the slightly increased J_{sc} resulting from the increased dye amount could not compensate for the significant loss of V_{oc} and *FF* owing to the intensified charge recombination.
[28] Z.-S. Wang, T. Yamaguchi, H. Sugihara, H. Arakawa, *Langmuir* **2005**, *21*, 4272.
[29] B. C. O'Regan, J. R. Durrant, *J. Phys. Chem. B* **2006**, *110*, 8544.
[30] Z.-S. Wang, M. Yanagida, K. Sayama, H. Sugihara, *Chem. Mater.* **2006**, *18*, 2912.